Transcriptomics and Functional Analysis of Graphene-Guided Osteogenic Differentiation of Mesenchymal Stem Cells

Long Wei LV[1], Yun Song LIU[1], Ping ZHANG[1], Ming GU[1], Xiang Song BAI[1], Chun Yang XIONG[2], Yong Sheng ZHOU[1]

Objective: *To explore graphene's effects on the gene expression profile of mesenchymal stem cells, and to reveal the mechanisms of graphene-guided osteogenic differentiation.*
Methods: *Human adipose-derived mesenchymal stem cells (hASCs) were cultured on single-layer graphene-coated titanium disks or titanium disks in proliferation medium (control) or osteoinduction medium for 7 days before RNA extraction. After library construction and RNA sequencing, identification of differentially expressed genes was performed through Limma package of R platform, with a cut-off value of log fold change (logFC) > = |1|. Pathway and Gene ontology (GO) analyses were conducted on DAVID Bioinformatics Resources 6.8 (NIAID/NIH). Network analyses were performed by the Ingenuity Pathways Analysis (IPA).*
Results: *Signalling pathway analysis revealed the top five pathways – cytokine-cytokine receptor interaction, neuroactive-ligand receptor interaction, calcium signalling pathway, PI3K-Akt signalling pathway and cell adhesion molecules. GO analyses demonstrated significant changes on cell adhesion, calcium signalling, and epigenetic regulation. IPA network analyses demonstrated that inflammation-related pathways were influenced by graphene, while the downstream factors of histone H3 and H4 were also altered especially under the existence of osteoinduction medium.*
Conclusion: *Graphene promotes osteogenic differentiation of hASCs mainly by influencing cell adhesion, cytokine-cytokine receptor interactions, inflammatory responses, and potentially influences histone H3 and H4 through epigenetic regulation.*
Key words: *bone tissue engineering, epigenetics, graphene, inflammation, RNA sequencing*
Chin J Dent Res 2018;21(2):101–111; doi: 10.3290/j.cjdr.a40436

1 Department of Prosthodontics, Peking University School and Hospital of Stomatology, National Engineering Laboratory for Digital and Material Technology of Stomatology, National Clinical Research Center for Oral Disease, Beijing Key Laboratory of Digital Stomatology, Beijing, P.R. China.
2 Department of Mechanics and Aerospace Engineering, College of Engineering, Peking University, Beijing, P.R. China.

Corresponding author: Dr Yong Sheng ZHOU, Department of Prosthodontics, Peking University School and Hospital of Stomatology, 22# Zhongguancun South Avenue, HaiDian District, Beijing 100081, P.R. China. Tel: 86 10 82195370; Fax: 86 10 62173402. Email: kqzhouysh@hsc.pku.edu.cn

This work was supported by the grant of Young Elite Scientist Sponsorship Program by CAST (2015QNRC001), and the grant (31600787, 81470769) from the National Natural Science Foundation of China, the Project for Culturing Leading Talents in Scientific and Technological Innovation of Beijing (Z171100001117169), the PKU School of Stomatology for Talented Young Investigators (PKUSS20150107).

Cell-surface interactions are believed to represent a promising management to precisely control seed cell function and differentiation in bone tissue engineering[1].

Therefore, biomaterial surface modification has attracted lots of attention. Although bone has the ability to repair minor injuries by remodelling, for large bone defects caused by severe trauma, congenital malformations, tumours and non-union fractures, remodelling is limited. Bone tissue engineering, which aims to regenerate bone, is a promising solution for these problems. Traditionally, bone tissue engineering consists of three factors, seed cells, scaffolds, and chemical osteoinductive factors[2]. Many researches employed chemical factors to induce differentiation *in vitro*, but guided differentiation of stem cells using these strategies is not

efficient and often requires a long cell culture time for maturation into osteogenic lineages. This has limited the widespread use of bone tissue engineering. Therefore, it is urgent to develop more efficient methods to enhance differentiation of mesenchymal stem cells (MSCs), and scaffold surface modification is likely to be a more convenient and stable manner[3].

Graphene, a 2D single-atomic-thick nanomaterial, holds great potential as coatings of bone implants and scaffolds, because it not only has exceptional mechanical, electronic, thermal properties, but also anti-bacteria and osteoinductive ability[4-7]. Single-layer graphene on copper foil can be produced in large scale by chemical vapour deposition (CVD) and then transferred to other substrates using polymethyl methacrylate (PMMA)[8-10]. Several studies have reported promising effects of graphene and its derivatives on cell adhesion, proliferation, and osteogenic differentiation[4-6,11]. In a previous study, we also confirmed that single-layer graphene could promote the osteogenic differentiation of human adipose-derived stem cells (hASCs) and human bone marrow-derived mesenchymal stem cells (hBMMSCs) *in vitro* and *in vivo*, and explored the underlying epigenetic mechanism in the fate of stem cells[12].

However, a clear view of graphene-cell interactions and its internal mechanisms is still incomplete. A few researches proposed various possible mechanisms of how graphene interacted with stem cells. Lee et al demonstrated that graphene and graphene oxide (GO) can accelerate MSC osteogenic differentiation as a result of preconcentration of osteogenic inducers, such as dexamethasone and β-glycerolphosphate, due to graphene's strong π–π stacking, hydrogen bonding, and electrostatic interactions with proteins[5]. Kim et al hypothesised that the unique nanotopography of the GO film would influence the formation of focal adhesions (FAs) and alter cell morphology[13]. Changes in cell adhesion and cell shape are important regulatory factors in stem cell lineage commitment[14]. Our previous researches revealed graphene's epigenetic role during the process of osteogenic differentiation and found that graphene accelerated the osteogenic differentiation of hASCs by enhancing the methylation level of histone H3 at lysine 4 (H3K4) at the promoter regions of osteogenic related genes[12]. However, a whole picture and the overall mechanisms of how graphene influences cell behaviours remains to be uncovered, and a clear mechanism is important for further graphene-related studies, safety evaluation and its future clinical applications.

Therefore, we investigated the response of hASCs to single-layer graphene on titanium substrate using the next generation sequencing bioinformatics approach. The changes on the whole gene expression profile will provide a more thorough picture to elucidate the regulatory network, and evaluate the safety and biocompatibility of graphene.

Materials and methods

Preparation of single-layer graphene sheets on titanium substrates

CVD grown single-layer graphene was purchased on a copper foil substrate from the American Chemical Society (ACS). Titanium (Ti) disks (23 mm × 23 mm for 6-well-plate cell culture, 10 mm × 10 mm for 24-well-plate cell culture, 99.6% purity, Leiden, Beijing, China) were cleaned in acetone, ethanol, and de-ionized water successively, each for 15 min using an ultrasonic cleaning machine. Graphene on copper foil was cut into optimal sizes to fit the sizes of Ti discs. For the transfer process, a PMMA thin film (950 K grade, 2 wt% in chlorobenzene) was spin-coated on the surface of graphene via a two-step process (step 1: 600 rpm for 10 s; step 2: 3000 rpm for 40 s) using a Laurell WS-400BZ-6NPP/LITE spin coater. After treatment at 180°C for 4 min, the copper foil substrate was then etched using $FeCl_3$ solution (0.05 g/mL in water), and the PMMA (top)/graphene (bottom) film floated to the surface of the solution. The film was rinsed twie with distilled water, and then a Ti disk was placed in de-ionized water with a tilting angle of 30 degrees underneath the floating film, and was picked up from the water with the coating of the graphene film. Finally, the thin PMMA film on the top of graphene was removed in an acetone bath for 30 min[12].

Atomic force microscopy (AFM) was used to confirm the presence of single-layer graphene on the Ti discs, and to measure surface roughness of the samples. Before AFM measurement, different samples were rinsed with ethanol and Milli-Q water, and then air-dried. The measurements were conducted under contact mode in dry conditions with a spring constant of 0.25 N/m, a scan rate of 1 Hz and a scan area of 3 μm × 3 μm. Measurements were run in triplicate for each sample.

Before using them for the cell culture, both graphene-coated Ti discs and the control group's smooth Ti discs were disinfected by soaking in 75% alcohol for 30 min.

hASCs culture and osteogenic induction

hASCs were purchased from ScienCell Company (San Diego, CA, USA). Dulbecco's modified Eagle's medium

(DMEM), foetal bovine serum (FBS), 100 × penicillin and streptomycin mixture were bought from Gibco (Grand Island, NY, USA). hASCs were cultured in fresh DMEM containing 10% (v/v) FBS, 100 U/mL penicillin G and 100 mg/mL streptomycin at 37°C in an incubator with an atmosphere consisting of 95% air, 5% CO_2 and 100% relative humidity. Cells at the fourth passage were used for the experiments. Osteoinduction medium (OM) comprised fresh DMEM containing 10% (v/v) FBS, 100 U/mL penicillin G and 100 mg/mL streptomycin (Sigma-Aldrich, St. Louis, MO, USA), 10nM dexamethasone (Sigma-Aldrich), 10 mM β-glycerophosphate, and 50 μg/ml L-ascorbic acid (Sigma-Aldrich).

Immunofluorescence

hASCs were seeded in 24-well plates on graphene or Ti surfaces. After 7 days of osteoinduction, samples were rinsed with PBS and fixed in 4% paraformaldehyde for 20 min at room temperature. Samples were then rinsed three times in PBS and post-fixed in 0.1% Triton X-100 for 15 min at room temperature. After another three lots of PBS rinsing, the samples were incubated overnight with 1:200 anti-osteocalcin primary antibodies (Santa Cruz, Dallas, TX, USA) at 4°C. Samples were rinsed and then incubated in 1:500 anti-rabbit secondary antibodies (4412S, Cell Signaling Technology, Beverly, MA, USA) for 1 h at room temperature. The samples were washed and incubated in 5μg/ml DAPI solution for 10 min at 37°C, before being visualised with a Confocal Zeiss Axiovert 650 microscope (Carl Zeiss Microimaging, Oberkochen, Germany), using the laser with wavelengths of 488 nm (green, osteocalcin) and 405 nm (blue, DAPI)[1].

RNA extraction, reverse transcription, and quantitative realtime PCR

hASCs were seeded in 6-well plates on graphene or Ti surfaces. Total cellular RNAs were isolated after 7 days of osteoinduction using the Trizol reagent (Invitrogen, Carlsbad, CA, USA) and used for first strand cDNA synthesis with the Reverse Transcription System (Roche, Basel, Switzerland). Quantifications of all gene transcripts were performed by quantitative real-time polymerase chain reaction (qPCR) using a Power SYBR Green PCR Master Mix and an ABI PRISM 7500 sequence detection system (Applied Biosystems, Foster City, CA, USA). The expression of *GAPDH* was detected as the internal control. The primers used were listed in Table 1. The cycle threshold values (Ct values) were used to calculate the fold differences by the ΔΔCt method[15].

RNA sequencing and bioinformatics

Total RNA was extracted from hASCs using the GeneJet RNA purification kit (Thermo Scientific). One μg RNA was used for sequencing library generation using the Truseq RNA Library Prep Kit V2 (Illumina) for mRNA seq according to the manufacturer's instructions. All libraries were sequenced on the NextSeq sequencer (Illumina) using the 35 nt paired-end sequencing protocol.

Differentially expressed gene (DEG) presenting a log fold change (logFC) $\geq |1|$, e.g. expression changes ≥ 2 or ≤ 0.5, was set to identify significant results. After we obtained the DEGs list, we performed Kyoto Encyclopedia of Genes and Genomes (KEGG) pathway analysis and Gene Ontology (GO) enrichment analyses, including biological processes (BP), cellular components (CC) and molecular functions (MF), associated with those DEGs through the online software DAVID Bioinformatics Resources 6.7 (https://david.ncifcrf.gov/)[16]. As for both KEGG and GO analyses, $P < 0.05$ were considered as significant, and the results were shown in $\log_{10}$ (P value). Additionally, we identified the enriched networks, molecular functions and pathways in the Ingenuity Pathways Analysis (IPA, Ingenuity Systems) platform via a license to Ingenuity Systems (www.ingenuity.com)[17].

Statistical analysis

All results were presented as mean ± standard deviation; the data were analysed using the SPSS 19.0 software (SPSS, Chicago, IL, USA) by one-way ANOVA plus Tukey test. For all tests, P values less than 0.05 were considered indicative of statistically significant differences.

Results

Surface characterisation

Atomic force microscope (AFM) observation (Fig 1A) demonstrated that there were many ripples and wrinkles on the surface of graphene-coated Ti. The roughness increased on graphene-coated Ti compared with smooth Ti substrate (Fig 1B). Therefore, graphene was transferred on Ti substrate successfully.

Enhanced osteogenic differentiation by graphene

OC expression detected by immunofluorescence showed that after 7 days of cell culture, hASCs in osteoinduction

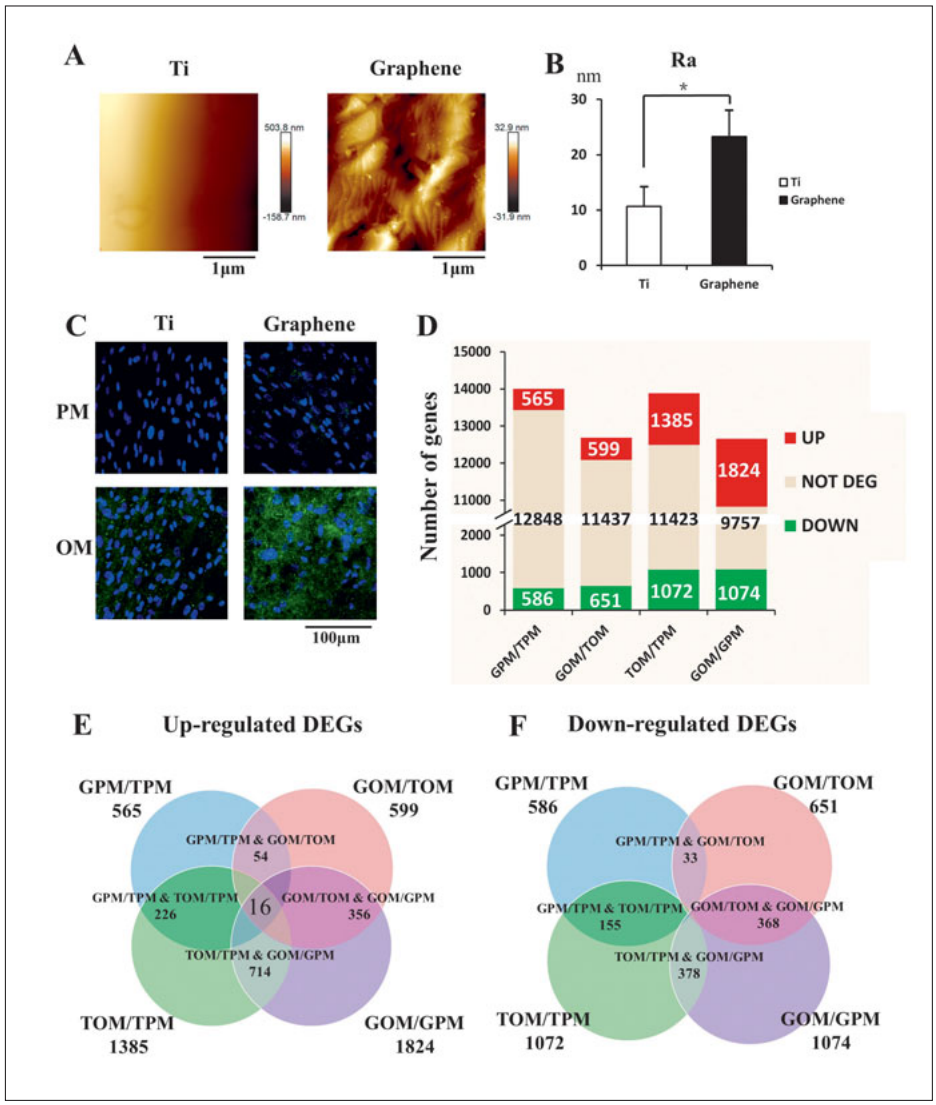

Fig 1 Surface characterisation and osteoinductive ability of graphene. **(A)** AFM images of graphene and Ti surface; **(B)** Roughness (Ra) analysis of graphene and Ti surface; **(C)** Immunofluorescent staining of osteocalcin (OCN) in hASCs cultured on graphene and Ti surfaces after 7 days of osteoinduction. OCN and nuclei are coloured green and blue respectively. (*$P < 0.05$). GPM: graphene with proliferation medium; GOM: graphene with osteoinduction medium; TPM: titanium with proliferation medium; TOM: titanium with osteoinduction medium.

medium (OM) cultured on graphene surface demonstrated obvious stronger OC-positive staining than Ti surface. As for hASCs cultured on a graphene surface in proliferation medium (PM), sporadic green fluorescence could be observed, while little green staining could be seen on Ti surface (Fig 1C).

Gene expression profile by RNA sequencing

To further investigate the overall mechanisms during the osteogenic process of graphene, gene expression profiles of hASCs cultured on graphene with proliferation medium (GPM), graphene with osteoinduction medium (GOM), Ti with proliferation medium (TPM), and Ti with osteoinduction medium (TOM) were analysed using RNA sequencing (RNA-seq). Differences of gene expression levels between graphene and titanium were compared: GPM versus TPM, GOM vs TOM. Differences of gene expression levels before and after osteoinduction were also compared: TOM vs TPM; GOM vs GPM. Statistics about DEG lists are summarised in Fig 1D. There were 565 upregulated DEGs and 586 downregulated DEGs when comparing GPM with TPM. There were 599 upregulated DEGs and 651 downregulated DEGs when comparing GOM with TOM. There were 1385 upregulated DEGs and 1072 downregulated DEGs when comparing TOM with TPM. There were 1824 upregulated DEGs and 1074 downregulated DEGs when comparing GOM with GPM (Fig 1D). Fig 1E demonstrated that the co-occurrence of upregulated DEGs in four cases was 16, and the co-occurrence of upregulated DEGs in both GPM/TPM and GOM/TOM

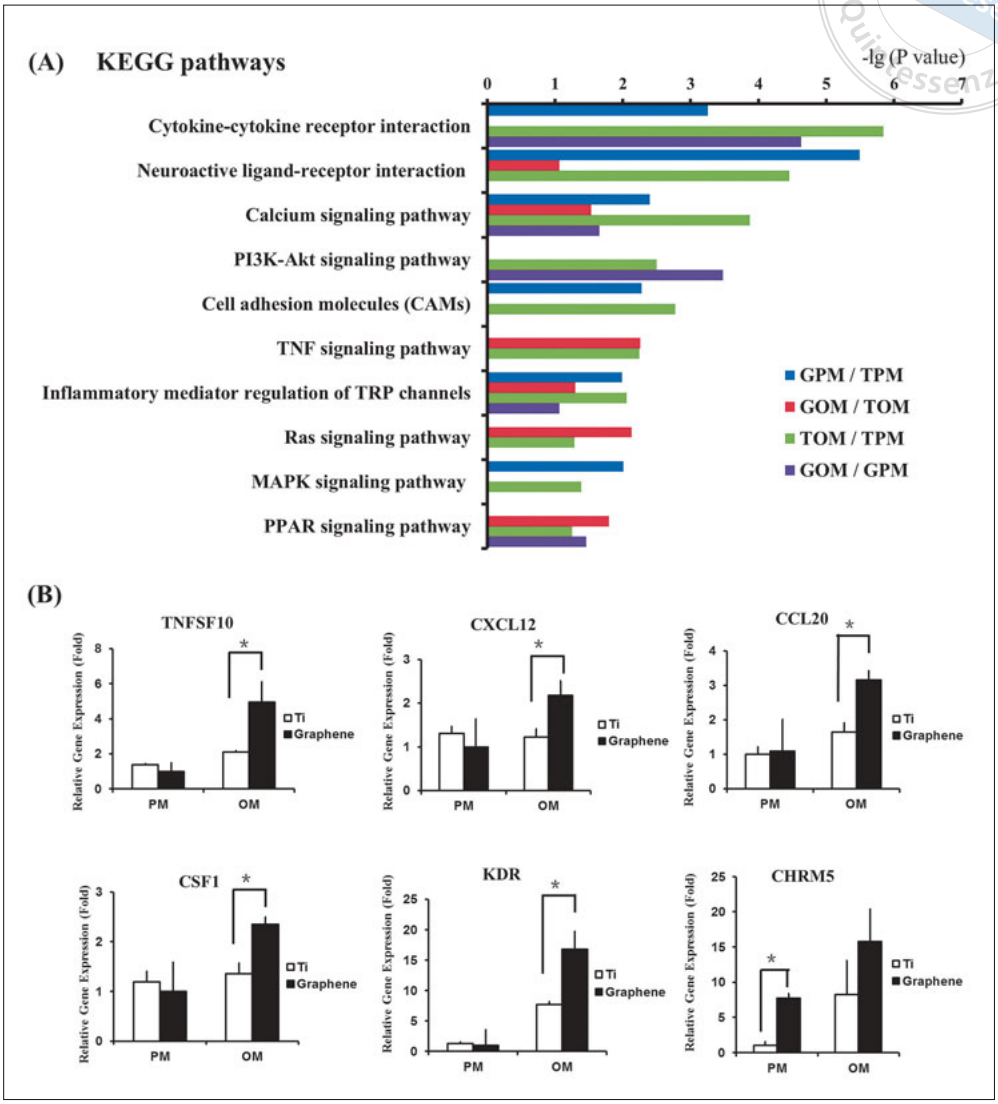

Fig 2 KEGG pathway analysis and verification of representative DEGs. **(A)** KEGG pathway analysis; **(B)** Verification of representative differentially expressed genes (DEGs) by realtime PCR. (*$P < 0.05$). Abbreviations as in Figure 1.

was 54. Fig 1F demonstrates that there was no co-occurrence of downregulated DEGs in four cases, while the co-occurrence of downregulated DEGs in both GPM/TPM and GOM/TOM was 33.

Kyoto encyclopedia of genes and genomes (KEGG) pathways analysis

Database of essential genes (DEG) annotations were conducted by DAVID (version 6.7) online software according to the information of the official gene symbol, and further analyses were performed on DEGs of annotated genes. KEGG analysis revealed that a significant proportion of DEGs intervened into cytokine-cytokine receptor interaction, neuroactive receptor interaction, calcium signalling pathways, PI3K-Akt (phosphatidylinositol 3 kinase, PI-3K; protein kinase B, PKB or Akt) signalling pathway, and cell adhesion molecules (Fig 2A). Upregulated genes and downregulated genes in cytokine-cytokine receptor interaction, neuroactive receptor interaction, calcium signalling pathways, and cell adhesion molecules are shown in Table 2.

Verification of representative DEGs by real-time PCR

Real-time PCR was used to confirm the expression level of six representative genes, which were significantly changed DEGs. TNFSF10 (TNF superfamily member 10), CCL20 (C-C motif chemokine ligand 20), CXCL12 (C-X-C motif chemokine ligand 12), CSF1 (colony stimulating factor 1), KDR (kinase insert domain receptor) expression was significantly increased after osteo-

Table 1 Primers for real-time PCR.

Gene	Forward primers	Reverse primers
GAPDH	GAAGGTGAAGGTCGGAGTC	GAAGATGGTGATGGGATTTC
TNFSF10	TCCGTCAGCTCGTTAGAAAGATGAT	GGTCCCAGTTATGTGAGCTGC
CXCL12	GCCCTTCAGATTGTAGCCCG	CTCGAGTGGGTCTAGCGGAA
CCL20	GCGAATCAGAAGCAGCAAGCA	TGCCGTGTGAAGCCCACAAT
CSF1	CTGCAGCGGCTGATTGACAG	TCTGAAGCGCATGGTGTCCT
KDR	AGCGGTCAACAAAGTCGGGA	TTTCAGGACCCCTGGTCACG
CHRM5	AACAAACCACTGCCAGGAACC	TGCAAGGCTGAGAATGATTTCCT

Table 2 Differentially expressed genes of hASCs on graphene vs titanium in proliferation medium by KEGG signalling pathway analysis.

KEGG pathways	Count	Upregulated genes	Downregulated genes
Cytokine-cytokine receptor interaction	25	11 TNFSF10, IL1R2, IL17B, IL23A, CNTF, TNFSF11, TNFSF15, IL6R, CXCL11, TNFSF18, TNFSF8	14 TNF, IL22RA1, IL7, TGFB3, CCL8, PF4, CNTFR, HGF, PF4V1, CCL7, TNFRSF11B, IFNE, BMPR1B, IL3RA
Neuroactive ligand-receptor interaction	34	18 RXFP4, PTGER4, GRIK2, OPRK1, RXFP2, DRD4, GNRHR, P2RX5, CRHR2, P2RX7, CHRM5, SSTR3, CHRM3, CHRNA9, CHRM2, P2RY2, CHRNA10, GRID1	16 F2RL3, PTGER1, CCKBR, GRIK1, GABRB3, PTH2R, FPR1, EDNRB, P2RY10, GPR35, SSTR2, MTNR1B, CHRNA5, HTR2C, PTAFR, CHRNG
Calcium signalling pathway	19	11 P2RX5, P2RX7, CHRM5, PLCE1, PLCB4, PDE1B, CHRM3, CHRM2, MYLK3, PLN, PLCB2	8 PTGER1, CCKBR, ITPKA, EDNRB, PLCG2, RYR2, HTR2C, PTAFR
Cell adhesion molecules (CAMs)	16	7 NRCAM, NCAM2, CD274, PECAM1, CLDN1, HLA-DRB5, ICOSLG	9 CLDN9, MPZ, ITGA8, NTNG1, CLDN10, ITGB2, JAM2, HLA-DMA, HLA-DRA

induction on graphene, while the difference between graphene and titanium in proliferation medium was not significant. CHRM5 (cholinergic receptor muscarinic 5) expression was significantly increased on graphene without osteoinduction.

Gene ontology analysis

Gene Ontology (GO) enrichment analyses, including biological process (BP), cellular component (CC) and molecular function (MF) were also performed by

Fig 3 Gene ontology analyses. **(A)** GO biological process analysis of GPM vs TPM; **(B)** GO biological process analysis of GOM vs TOM; **(C)** GO cellular component analysis of GPM vs TPM; **(D)** GO cellular component analysis of GOM vs TOM; **(E)** GO molecular function analysis of GPM vs TPM; **(F)** GO molecular function analysis of GOM vs TOM. Abbreviations as in Figure 1.

DAVID online software. According to GO analyses of GPM vs TPM, cell adhesion, cytoskeleton, cell metabolism, and cellular interactions, as well as calcium pathway and mineralization were significantly influenced ($P < 0.05$, -lg P > 1.3) by graphene (Figs 3A, C and E). On the other hand, as for GOM vs TOM, graphene not only influenced cell adhesion, cytoskeleton, cell metabolism, cellular interactions, and calcium pathway, but also impacted cell nucleus and epigenetic regulation (Figs 3B, D and F).

Network analysis

Network analysis between GPM and TPM by IPA demonstrated that inflammation-related signalling pathways including NF-κB, P38-MAPK, and Jnk were likely to

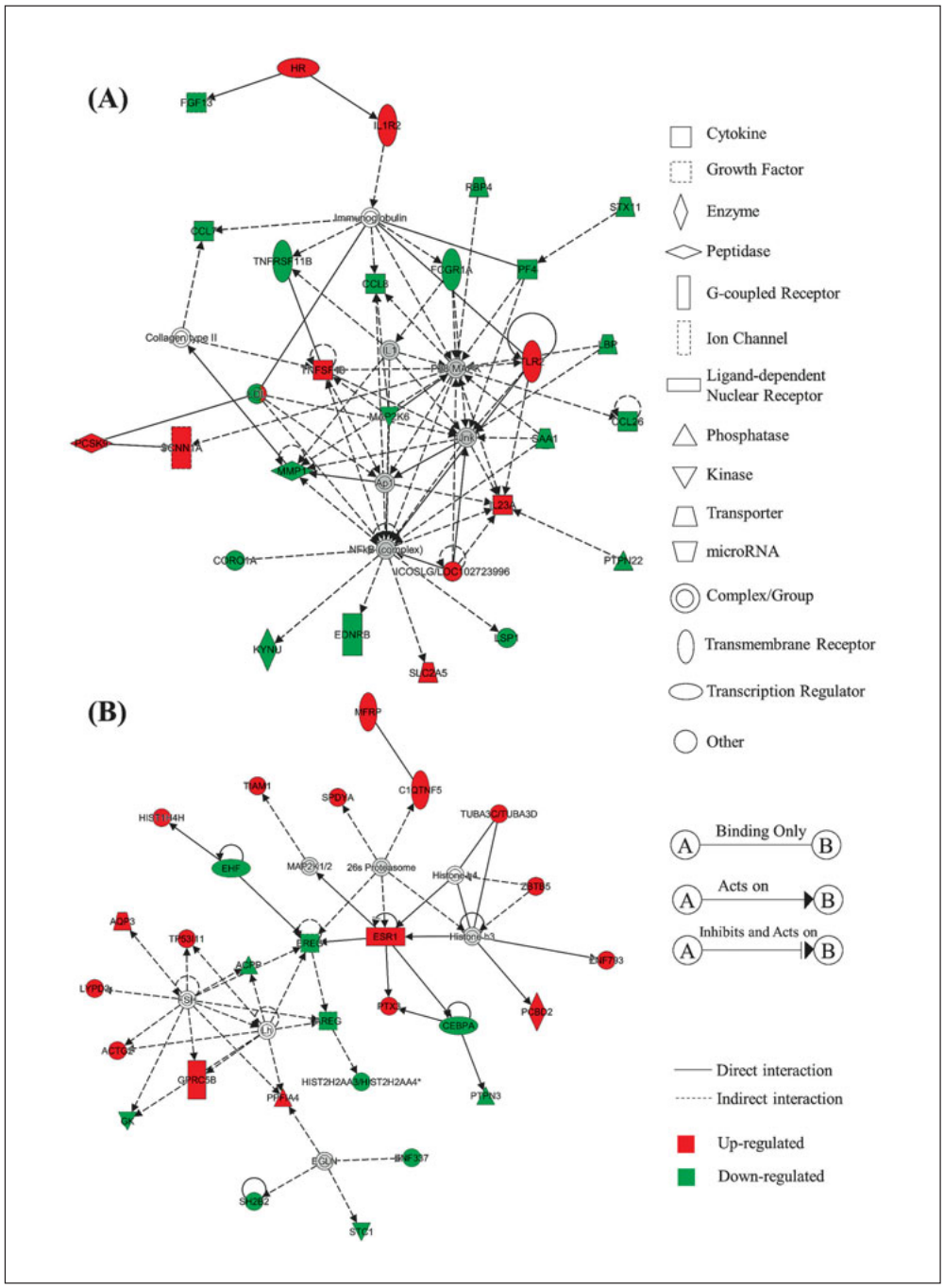

Fig 4 IPA network analyses. **(A)** IPA network of GPM vs TPM; **(B)** IPA network of GOM vs TOM. Abbreviations as in Figure 1.

be associated with this process. Potential downstream factors, including CORO1A (coronin 1A), KYNU (kynureninase), EDNRB (endothelin receptor type B), LSP1 (lymphocyte-specific protein 1) of NF-κB, were down regulated, while SLC2A5 (solute carrier family 2 member 5) was upregulated (Fig 4A).

Meanwhile, we found that the downstream factors of histone H3, H4, including TUBA3C/D (tubulin alpha 3c/d), ZBTB5 (zinc finger and BTB domain containing 5), ZNF793 (zinc finger protein 793), PCBD2 (pterin-4 alpha-carbinolamine dehydratase 2), estrogen receptor 1, were upregulated by graphene under the existence of osteoinduction medium. Therefore, graphene may regulate cell functions through an epigenetic network (Fig 4B). And these results of IPA network analyses were in consistent with that of GO analyses, confirming the role of graphene on epigenetic regulation under the existence of OM.

Discussion

In this study, we successfully transferred single-layer graphene from Cu substrate to Ti substrate, providing a potential and wide application of surface modification method for Ti-based bone implants and medical devices. We found that single-layer graphene on Ti substrate accelerated osteogenic differentiation of hASCs compared with pure Ti. RNA sequencing and bioinformatics analyses revealed that graphene mainly influenced cell adhesion, cytokine-cytokine receptor interactions, inflammatory responses, and calcium signalling pathways. Moreover, epigenetic regulation was also involved in graphene-guided osteogenic differentiation of hASCs.

Cell adhesion, the beginning of cell-surface interactions

The minute a cell adheres to the substrate, their interactions begin. The cell spreads and thus cell shape changes under the guidance of material substrate. Material topography, adhesiveness, and 3D-dimensionality will all lead to reorganisation of the cytoskeleton. Forces generated by the cytoskeleton components including actin and myosin can be transmitted to the nucleus via physical links on the nuclear envelope[18]. And cell morphology and nuclear deformation are important factors to guide cell functions, including cell proliferation and lineage commitment[19,20]. Meanwhile, these influences are relayed by adhered cells to surrounding cells through cell synapse and cell-cell junctions, as well as secretion of cytokines or exosomes into extracellular region. In this research, we found that cell adhesion molecules and PI3K-Akt pathway were significantly influenced by graphene according to KEGG pathway analysis (Fig 2A). Meanwhile, GO analyses also revealed significant changes in plasma membrane, cytoskeleton, and thus influencing transmembrane transport, extracellular matrix, cell-cell junction, and cell-cell signalling transduction (Fig 3). Therefore, graphene-guided osteogenic differentiation begins from cell adhesion and changes in cell morphology, and is extended to surrounding cells through cell-cell junctions and alterations in the microenvironment of residing cells.

Inflammatory response, inevitable and indispensable process for bone regeneration

The process of bone repair begins from inflammatory responses[21]. In the past, inflammation was viewed as a negative factor of bone regeneration. On the contrary, inflammation and immune response is indispensable in new bone formation, since the essence of bone regeneration is a balance between osteogenesis and bone resorption. Biomaterials can exert profound impacts on the host immune response, thus the concept has emerged to design biomaterials that can trigger desired immunological outcomes and support the healing process[22]. However, engineering immune-modulating biomaterials requires an in-depth understanding of the host inflammatory and wound healing response to implanted materials. Fortunately, high throughput experiments provide a promising resolution. In this study, cytokine-cytokine receptor interactions were significantly influenced by graphene according to KEGG pathway analysis, leading to upregulation of cytokines including TNFSF10, CCL20, CXCL12, CSF1, KDR and CHRM5 as verified by real-time PCR (Fig 2). Meanwhile, downstream factors of NF-κB, P38-MAPK, and Jnk were mainly downregulated according to IPA network analysis (Fig 4A). These results provide a more thorough insight into the inflammation process of how graphene interacts with host cells.

Epigenetic regulation, non-negligible mechanism in cell-material interactions

Epigenetic regulation plays an important role in cell functions[14]. Epigenetics refers to heritable changes in gene expression pattern that do not alter the DNA sequence. The epigenome helps to stabilise cell status, which can be altered during stem cell differentiation and somatic cell reprogramming[23]. Interestingly, biomaterial cues, which act as outside signals, can influence the internal epigenetic state through various epigenetic regulatory mechanisms, including DNA methylation, chromatin remodelling, and non-coding RNAs. Our research group found that graphene promoted osteogenic differentiation of hASCs by enhancing H3K4 methylation level at the promoter regions of osteogenic related genes through inhibiting histone demethylase retinoblastoma protein 2 (RBP2)[12]. Meanwhile, graphene can also improve cellular reprogramming efficiency by inducing a mesenchymal-to-epithelial transition (MET) process, which is known to affect H3K4me3 levels[24]. In this research, we found that graphene influenced an epigenetic-related process, including nuclear inner membrane, nuclear envelop, DNA binding, nucleic acid binding, β-catenin binding, and DNA templated as well as transcription under the existence of OM (Figs 3B, D and F). Meanwhile, histone H3, H4 related regulators were significantly altered by graphene, demonstrating graphene's potential regulatory network through epigenetic regulation (Fig 4B). Compared with small-molecule drugs, using biomaterials to direct cell behaviours is safer and

therefore more promising in the clinical use of human cells.

Meanwhile, epigenetic regulation exerted by biomaterials on the biological effects of stem cells not only plays an important role in regenerative medicine, but is also a potential set of tools for biomaterial safety evaluation[25-27]. Epigenetic alteration is a mechanism, which explains the long-lasting and memorable effects of cells directed by biomaterial cues. Meanwhile, epigenetic regulation is an important process, which breaks through the barrier of cell lineage commitment. The assessment of epigenetic effects may also be approached as new model systems that can directly assess transgenerational effects or potentially sensitive stem cell populations. These will expand the scope of safety assessment tools for evaluating new materials.

Perspectives and applications

Graphene is a promising material for the coating of bone implants and medical devices. It is only one-atom thick, thus introducing the least amount of artificial material in surface modification. Meanwhile, it enjoys a large number of remarkable properties, including exceptional mechanical, electronic, and thermal properties[28]. Specifically, graphene has the highest Young's modulus (0.5-1TPa) among any known material, so it is not brittle[29,30]. Moreover, graphene can be transferred onto any flat or irregular-shaped surface[31]. These extraordinary properties make graphene a promising choice as a component of scaffold material or a potential surface modification in bone tissue engineering. By utilising the novel method of next generation sequencing, an overall picture of graphene's regulating mechanism has been drawn, thus providing potent evidence for future clinical application of graphene in the field of bone tissue engineering.

Conclusions

Single-layer graphene on titanium substrate promotes osteogenic differentiation of hASCs. RNA sequencing and bioinformatics analyses reveal that the underlying mechanisms mainly relate to cell adhesion, cytokine-cytokine receptor interactions, inflammatory responses, and calcium signalling pathways. Moreover, graphene potentially regulates the state of histone H3, H4 through an epigenetic regulatory network.

Conflicts of interest

The authors reported no conflicts of interest related to this study.

Author contribution

Dr Long Wei LV designed the study, performed experiments, collected and analysed data, interpreted results, and prepared the manuscript; Drs Yun Song LIU and Ping ZHANG performed experiments, analysed data and interpreted the results; Drs Ming GU and Xiang Song BAI performed experiments, collected and analysed data; Dr Chun Yang XIONG designed the study and revised the manuscript; Dr Yong Sheng ZHOU designed the study, analysed data, interpreted results, and critically revised the manuscript.

(Received Nov 6, 2017; accepted Jan 3, 2018)

References

1. Lv L, Liu Y, Zhang P, et al. The nanoscale geometry of TiO_2 nanotubes influences the osteogenic differentiation of human adipose-derived stem cells by modulating H3K4 trimethylation. Biomaterials 2015;39:193–205.
2. Henkel J, Woodruff MA, Epari DR, et al.. Bone Regeneration Based on Tissue Engineering Conceptions – A 21st Century Perspective. Bone Res 2013;1:216–248.
3. Gu M, Liu Y, Chen T, et al. Is graphene a promising nano-material for promoting surface modification of implants or scaffold materials in bone tissue engineering? Tissue Eng Part B Rev 2014;20:477–491.
4. Nayak TR, Andersen H, Makam VS, et al. Graphene for controlled and accelerated osteogenic differentiation of human mesenchymal stem cells. ACS Nano 2011 28;5:4670–4678.
5. Lee WC, Lim CH, Shi H, et al. Origin of enhanced stem cell growth and differentiation on graphene and graphene oxide. ACS Nano 2011;5:7334–7341.
6. Talukdar Y, Rashkow J, Lalwani G, Kanakia S, Sitharaman B. The effects of graphene nanostructures on mesenchymal stem cells. Biomaterials 2014;35:4863–4877.
7. Some S, Ho SM, Dua P, et al. Dual functions of highly potent graphene derivative-poly-L-lysine composites to inhibit bacteria and support human cells. ACS Nano 2012;6:7151–7161.
8. Zhang Y, Zhang L, Zhou C. Review of chemical vapor deposition of graphene and related applications. Acc Chem Res 2013;46: 2329–2339.
9. Reina A, Jia X, Ho J, et al. Large area, few-layer graphene films on arbitrary substrates by chemical vapor deposition. Nano Lett 2009;9: 30–35.
10. Grandthyll S, Gsell S, Weinl M, Schreck M, Hüfner S, Müller F. Epitaxial growth of graphene on transition metal surfaces: chemical vapor deposition versus liquid phase deposition. J Phys Condens Matter 2012;24:314204.
11. Qiu J, Geng H, Wang D, et al. Layer-Number Dependent Antibacterial and Osteogenic Behaviors of Graphene Oxide Electrophoretic Deposited on Titanium. ACS Appl Mater Interfaces 2017;9: 12253–12263.
12. Liu Y, Chen T, Du F, et al. Single-Layer Graphene Enhances the Osteogenic Differentiation of Human Mesenchymal Stem Cells In Vitro and In Vivo. J Biomed Nanotechnol 2016;12:1270–1284.
13. Kim J, Choi KS, Kim Y, et al..Bioactive effects of graphene oxide cell culture substratum on structure and function of human adipose-derived stem cells. J Biomed Mater Res A 2013;101:3520–3530.
14. Lv L, Tang Y, Zhang P, Liu Y, Bai X, Zhou Y. Biomaterial Cues Regulate Epigenetic State and Cell Functions-A Systematic Review.

Tissue Eng Part B Rev 2017 Oct 19. doi: 10.1089/ten.teb.2017.0287. [Epub ahead of print]
15. Lv L, Ge W, Liu Y, et al. Lysine-specific demethylase 1 inhibitor rescues the osteogenic ability of mesenchymal stem cells under osteoporotic conditions by modulating H3K4 methylation. Bone Res 2016;4:16037.
16. Huang da W, Sherman BT, Lempicki RA. Systematic and integrative analysis of large gene lists using DAVID bioinformatics resources. Nat Protoc 2009;4:44–57.
17. Juss J, Herre J, Begg M, et al. Genome-wide transcription profiling in neutrophils in acute respiratory distress syndrome. Lancet 2015;385:S55.
18. Jain N, Iyer KV, Kumar A, Shivashankar GV. Cell geometric constraints induce modular gene-expression patterns via redistribution of HDAC3 regulated by actomyosin contractility. Proc Natl Acad Sci US 2013;110:11349–11354.
19. Talwar S, Jain N, Shivashankar GV. The regulation of gene expression during onset of differentiation by nuclear mechanical heterogeneity. Biomaterials 2014;35:2411–2419.
20. Badique F, Stamov DR, Davidson PM, et al. Directing nuclear deformation on micropillared surfaces by substrate geometry and cytoskeleton organization. Biomaterials 2013;34:2991–3001.
21. Hadjidakis DJ, Androulakis II. Bone remodeling. Ann N Y Acad Sci 2006;1092:385–396.
22. Franz S, Rammelt S, Scharnweber D, Simon JC. Immune responses to implants – a review of the implications for the design of immunomodulatory biomaterials. Biomaterials 2011;32:6692–6709.
23. Bintu L, Ishibashi T, Dangkulwanich M, et al. Nucleosomal elements that control the topography of the barrier to transcription. Cell 2012;151:738–749.
24. Yoo J, Kim J, Baek S, Park Y, Im H, Kim J. Cell reprogramming into the pluripotent state using graphene based substrates. Biomaterials 2014;35:8321–8329.
25. Miousse IR, Currie R, Datta K, et al. Importance of investigating epigenetic alterations for industry and regulators: An appraisal of current efforts by the Health and Environmental Sciences Institute. Toxicology 2015;335:11–19.
26. Dearfield KL, Gollapudi BB, Bemis JC, et al. Next generation testing strategy for assessment of genomic damage: A conceptual framework and considerations. Environ Mol Mutagen 2017;58:264–283.
27. Igarashi K, Ideta-Otsuka M, Narita M. The Current State and Future Development of Epigenetic Toxicology [Article in Japanese]. Yakugaku Zasshi 2017;137:265–271.
28. Geim AK. Graphene: status and prospects. Science 2009;324:1530–1534.
29. Garcia-Sanchez D, van der Zande AM, Paulo AS, Lassagne B, McEuen PL, Bachtold A. Imaging mechanical vibrations in suspended graphene sheets. Nano Lett 2008;8:1399–1403.
30. Lee C, Wei X, Kysar JW, Hone J. Measurement of the elastic properties and intrinsic strength of monolayer graphene. Science 2008;321:385–388.
31. Lee Y, Bae S, Jang H, et al. Wafer-scale synthesis and transfer of graphene films. Nano Lett 2010;10:490–493.